Molecular Cell
Article

Global Analysis of Eukaryotic mRNA Degradation Reveals Xrn1-Dependent Buffering of Transcript Levels

Mai Sun,[1,3] Björn Schwalb,[1,3] Nicole Pirkl,[1] Kerstin C. Maier,[1] Arne Schenk,[1] Henrik Failmezger,[1,2] Achim Tresch,[1,2,*] and Patrick Cramer[1,*]

[1]Gene Center Munich and Department of Biochemistry, Center for Integrated Protein Science CIPSM, Ludwig-Maximilians-Universität München, Feodor-Lynen-Strasse 25, 81377 Munich, Germany

[2]Present address: Max Planck Institute for Plant Breeding Research, Carl-von-Linné-Weg 10, 50829 Cologne, Germany, and University of Cologne, Botanical Institute III, Zuelpicher Strasse 47b, 50674 Cologne, Germany

[3]These authors contributed equally to this work

*Correspondence: tresch@mpipz.mpg.de (A.T.), cramer@lmb.uni-muenchen.de (P.C.)

http://dx.doi.org/10.1016/j.molcel.2013.09.010

SUMMARY

The rates of mRNA synthesis and degradation determine cellular mRNA levels and can be monitored by comparative dynamic transcriptome analysis (cDTA) that uses nonperturbing metabolic RNA labeling. Here we present cDTA data for 46 yeast strains lacking genes involved in mRNA degradation and metabolism. In these strains, changes in mRNA degradation rates are generally compensated by changes in mRNA synthesis rates, resulting in a buffering of mRNA levels. We show that buffering of mRNA levels requires the RNA exonuclease Xrn1. The buffering is rapidly established when mRNA synthesis is impaired, but is delayed when mRNA degradation is impaired, apparently due to Xrn1-dependent transcription repressor induction. Cluster analysis of the data defines the general mRNA degradation machinery, reveals different substrate preferences for the two mRNA deadenylase complexes Ccr4-Not and Pan2-Pan3, and unveils an interwoven cellular mRNA surveillance network.

INTRODUCTION

Cellular mRNA levels govern genome expression. The level of an mRNA is determined by its synthesis rate (SR) and its degradation rate (DR). Recent work showed that mRNA levels in eukaryotic cells are maintained close to normal values, i.e., buffered, when SRs or DRs are perturbed by mutations that impair nuclear mRNA synthesis or cytoplasmic mRNA degradation, respectively (Shalem et al., 2008, 2011; Bregman et al., 2011; Pérez-Ortín et al., 2012; Sun et al., 2012; Trcek et al., 2011; Pai et al., 2012). In the yeast *Saccharomyces cerevisiae*, a mutation in the transcribing enzyme RNA polymerase II (Pol II) leads to a global decrease of SRs that is compensated by a decrease in DRs, resulting in a buffering of mRNA levels (Sun et al., 2012). Vice versa, a decrease in DRs caused by the deletion of the gene encoding the mRNA degradation enzyme Ccr4 is compensated by a decrease in SRs (Sun et al., 2012).

The mechanisms underlying the buffering of mRNA levels remain unknown. Kinetic modeling indicated that the buffering may depend on a putative factor that acts positively on mRNA degradation and negatively on mRNA synthesis (Sun et al., 2012). To search for such a factor, we analyzed 46 mutant yeast strains that lacked mRNA degradation factor genes with the use of comparative dynamic transcriptome analysis (cDTA) (Sun et al., 2012). cDTA is based on metabolic labeling of newly transcribed RNA by 4-thiouracil (4sU) in yeast (Miller et al., 2011) and allows for normalization between wild-type and mutant strains, thus enabling a global monitoring of SR and DR changes upon perturbation (Sun et al., 2012). Our factor search was based on the rationale that deletion of a degradation factor would result in changes in both DRs and SRs and mRNA level buffering unless the factor is required for buffering of mRNA levels.

Degradation of eukaryotic mRNAs has been extensively studied (Garneau et al., 2007; Parker and Sheth, 2007). mRNA degradation generally commences with a shortening of the 3′-poly(A) (pA) tail (deadenylation) (Collart, 2003; Yamashita et al., 2005), followed by removal of the 5′-cap (decapping) (Coller and Parker, 2004; Franks and Lykke-Andersen, 2008). mRNAs are then degraded in 5′-3′ direction by the Xrn1 exonuclease (Houseley and Tollervey, 2009) and in 3′-5′ direction by the exosome (Lebreton and Séraphin, 2008). When the pA tail reaches a critical length, mRNAs are subjected to decapping by Dcp2 (Muhlrad et al., 1994), which is promoted by Dcp1 and Edc3 (Kshirsagar and Parker, 2004), the yeast-specific factors Edc1 and Edc2 (Dunckley et al., 2001), and the translation-repressing factors Dhh1 (Coller and Parker, 2005), Pat1, and the Lsm complex (Chowdhury et al., 2007; Pilkington and Parker, 2008). Cytoplasmic mRNA degradation is coupled to mRNA translation (Hu et al., 2009). Dedicated transcription- and translation-coupled quality surveillance pathways also contribute to mRNA degradation (Schmid and Jensen, 2010; Shoemaker and Green, 2012; Shyu et al., 2008).

In our analysis we included factors involved in deadenylation (Ccr4, Pop2/Caf1, Caf40, Not3, Pan2, and Pan3) and exonucleases required for bulk mRNA degradation (Xrn1 and the exosome subunits Rrp6 and Rrp47/Lrp1). We also included factors

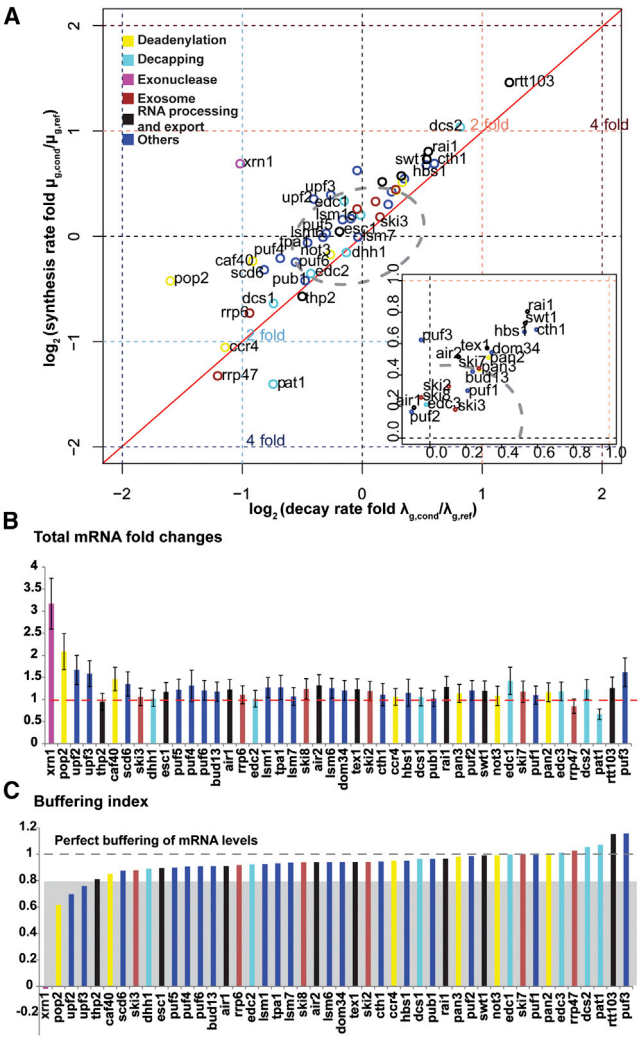

Figure 1. Global cDTA of mRNA Degradation Reveals Generality of mRNA Level Buffering

(A) Scatter plot showing global changes in mRNA DRs (log fold of median mRNA decay rates in mutant versus wild-type, x axis) and SRs (log fold of median mRNA synthesis rates in mutant versus wild-type, y axis) in 46 yeast deletion strains. The center of each circle is determined by the median DR and SR of the strain. The gray ellipse indicates the 95% confidence region. See also Figure S1.

(B) Bar plot depicting changes in global mRNA level in 46 yeast deletion strains. An mRNA level change of 1 indicates that global mRNA levels of the mutant and wild-type strains are the same. The error bars indicate the standard deviation calculated from the replicate measurements.

(C) Bar plot depicting the buffering index (BI). BI is 1 when mRNA level buffering is perfect. BI is between 0 and 1 when mRNA level buffering is partial. BI of 0 or below 0 indicates that there is no mRNA level buffering.

that target decapping substrates (Lsm1, Lsm6, and Lsm7), decapping enhancers (Edc1, Edc2, Edc3, Dhh1, Pat1, and Scd6), scavenger decapping factors (Dcs1 and Dcs2), and exosome-associated factors (Ski2, Ski3, Ski8, and Ski7). We further included factors involved in transcription termination, nuclear RNA surveillance, and splicing (Rtt103, Rai1, Air1, Air2, Esc1, and Bud13), factors that bind RNA elements and regulate mRNA degradation (Puf1/Jsn1, Puf2, Puf3, Puf4, Puf5/Mpt5, Puf6, Pub1, Tpa1, and Cth1), factors involved in mRNA export (Thp2 and Tex1), factors implicated in translation surveillance (Dom34, Hbs1, Upf2/Nmd2, and Upf3), and an endonuclease (Swt1).

The resulting cDTA data sets for 46 yeast deletion strains each contain SRs and DRs for about 4,300 mRNAs. All mutant strains showed a buffering of mRNA levels, with one marked exception, the strain lacking the exonuclease Xrn1. We therefore analyzed mutants of Xrn1 to elucidate its role in the buffering of mRNA levels. Correlation analysis of DR changes in mutant strains recapitulated known interactions between degradation factors and unraveled new ones. Our results provide a rich resource for studying mRNA metabolism and identify Xrn1 as a key factor required for the buffering of mRNA levels in a eukaryotic cell. While this manuscript was in revision, a paper was published that also reported a buffering of transcript level upon perturbation of mRNA degradation (Haimovich et al., 2013). We compare these new data to our results in the Discussion.

RESULTS

Global Analysis of mRNA Degradation

We gathered cDTA data from *Saccharomyces cerevisiae* BY4741 strains during logarithmic growth in YPD media (Table S1). Strains were verified by PCR and growth on selective media (Experimental Procedures). cDTA was carried out as described (Sun et al., 2012). Briefly, RNA was metabolically labeled with 4sU for 6 min, and 2.25×10^8 cells were mixed with 0.75×10^8 cells from labeled *Schizosaccharomyces pombe* culture that provided an internal standard. Strain ploidy was analyzed by plotting the levels of total RNA per chromosome (Figure S1). This uncovered nine aneuploid mutant strains, six of which we could regenerate with normal ploidy, whereas the others had to be excluded. For strains that showed more than a 2-fold difference in total RNA, chromosome copy number was analyzed by FACS and polyploid strains were excluded. From each strain, at least two biological replicates were measured. The Spearman correlation of replicate measurements was always close to 1. With the use of our previously described algorithm (Sun et al., 2012), we obtained a high-quality data set including for each strain the median SR and DR (Table S2), the total mRNA levels (Table S3), the SRs based on labeled mRNA (Table S4), and the DRs (Table S5).

Generality of mRNA Level Buffering

When we plotted the changes in median SRs against changes in median DRs for each mutant strain (Table S2), the data points scattered along the main diagonal (Figure 1A). Thus, changes in DRs that were induced upon mutation were generally compensated by changes in SRs. To assign a significance level to these changes, we fitted a bivariate Gaussian distribution to the pooled median SR and DR estimates of a total of 228 *S. cerevisiae* samples after normalization to their *S. pombe* references, including 18 biological wild-type replicates. Data points outside the resulting 95% confidence region (gray ellipse in Figure 1A) indicate significant changes in global SR and/or DR, since they do not result from random fluctuations. The high precision of our

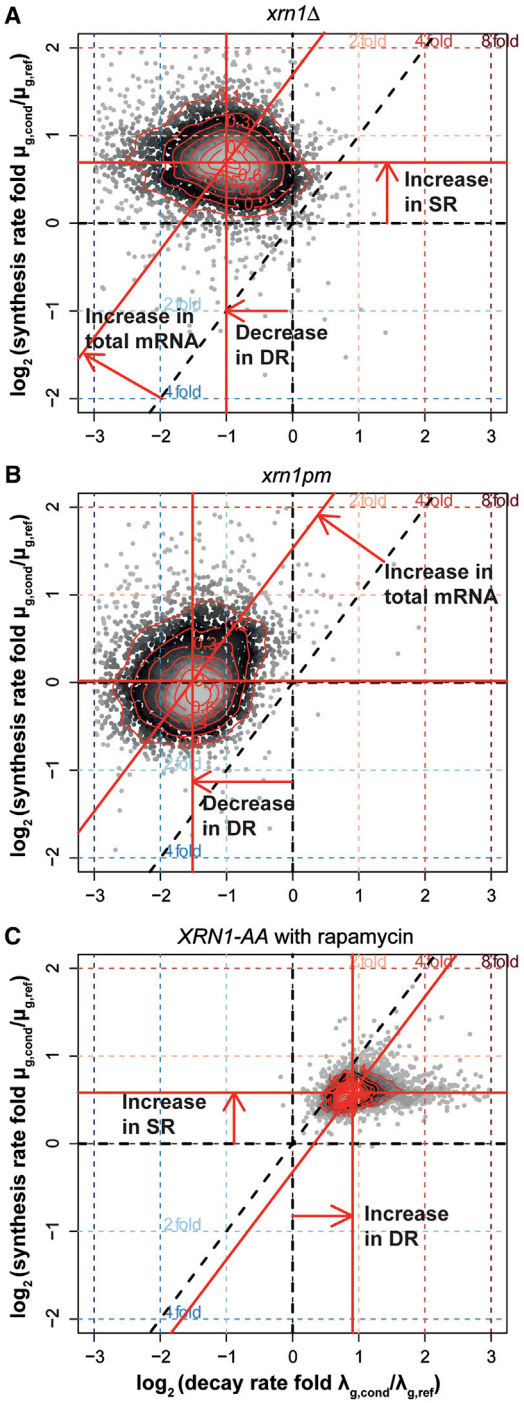

Figure 2. mRNA Level Buffering Requires Xrn1 Activity

(A) Scatter plot with changes in mRNA SRs (log fold, y axis) and DRs (log fold, x axis) in the *xrn1Δ* deletion strain. Each point corresponds to one mRNA. The density of points is encoded by their brightness (gray scale). Contour lines define regions of equal density. A global shift in the median DR is indicated by the shift of the horizontal red line relative to the dashed x axis line. Arrows indicate change in global SR (vertical), DR (horizontal), and mRNA level (diagonal).

(B) Scatter plot as in (A) but for the *xrn1pm* strain relative to its isogenic wild-type strain *XRN1*.

(C) Scatter plot as in (A) and (B) but showing the changes in the *XRN1AA* strain after treatment with rapamycin compared to the untreated strain. See also Figure S2.

measurements revealed even mild effects of most mutations under optimum growth conditions (standard deviation for changes in SR is 0.22 and for changes in DR is 0.24). Of the 46 strains analyzed, 7 showed strong effects with median SR or DR changes above 2-fold, whereas 16 strains did not show significant rate changes. Most strains maintained similar mRNA levels (Figure 1B), demonstrating the generality of mRNA level buffering.

mRNA Level Buffering Requires Xrn1 Activity

The analysis revealed a single strong outlier, the strain lacking the exonuclease Xrn1 (Figure 1). In this strain, the median DR was decreased by 2-fold relative to wild-type, but the median SR was increased by 1.6-fold. As a result, mRNA levels increased 3.2-fold (Figure 1B), showing that the buffering mechanism was defective. Thus, Xrn1 mediates global mRNA degradation as expected, but its absence showed an unexpected positive effect on mRNA synthesis rather than a negative effect that would be required for buffering. The apparent repression of mRNA synthesis cannot be explained by stabilization of labeled RNAs, since our SR estimator accounts for the degradation of labeled RNA.

To quantify the mRNA buffering capacity of mutant strains, we introduced the buffering index (BI), which is calculated as follows:

$$BI = 1 - \frac{(T_{mutant} - T_{wt})}{(T_{theoretical} - T_{wt})}$$

In this equation, T_{mutant} and T_{wt} are the measured median total mRNA levels of the mutant and the wild-type, respectively. $T_{theoretical}$ is the theoretically obtained total RNA level that would result from impaired degradation but unaffected synthesis, i.e., in the absence of buffering. The ratio $(T_{mutant} - T_{wt}) / (T_{theoretical} - T_{wt})$ measures the change in total mRNA relative to the expected change assuming no buffering. Thus, the BI measures the fraction of the expected total mRNA change that has been buffered. A BI of 1 indicates perfect buffering, i.e., changes in DR are entirely compensated by changes in SR. Out of the 46 mutant strains, 42 showed a BI above 0.8, 3 showed a BI between 0.6 and 0.8, and only the *xrn1Δ* mutant had a BI close to zero (Figure 1C). Xrn1 thus exhibits the features predicted for a factor involved in mRNA buffering; it is an mRNA degradation factor with a negative effect on mRNA synthesis (Sun et al., 2012).

To investigate the role of Xrn1 in the buffering mechanism, we prepared a yeast strain (*xrn1pm*) with two point mutations in the Xrn1 active site (D206A, D208A) that abolish exonuclease activity (Solinger et al., 1999). We collected a cDTA profile for the *xrn1pm* strain and compared it to an isogenic wild-type strain (Experimental Procedures). The median DR was decreased to 36%, similar as in the *xrn1Δ* strain, but the median SR remained unchanged, leading to a 2.6-fold increase in total mRNA levels (Figures 2A and 2B). These results demonstrate that the catalytic activity of Xrn1 is responsible for the decrease in DRs and is required for mRNA level buffering.

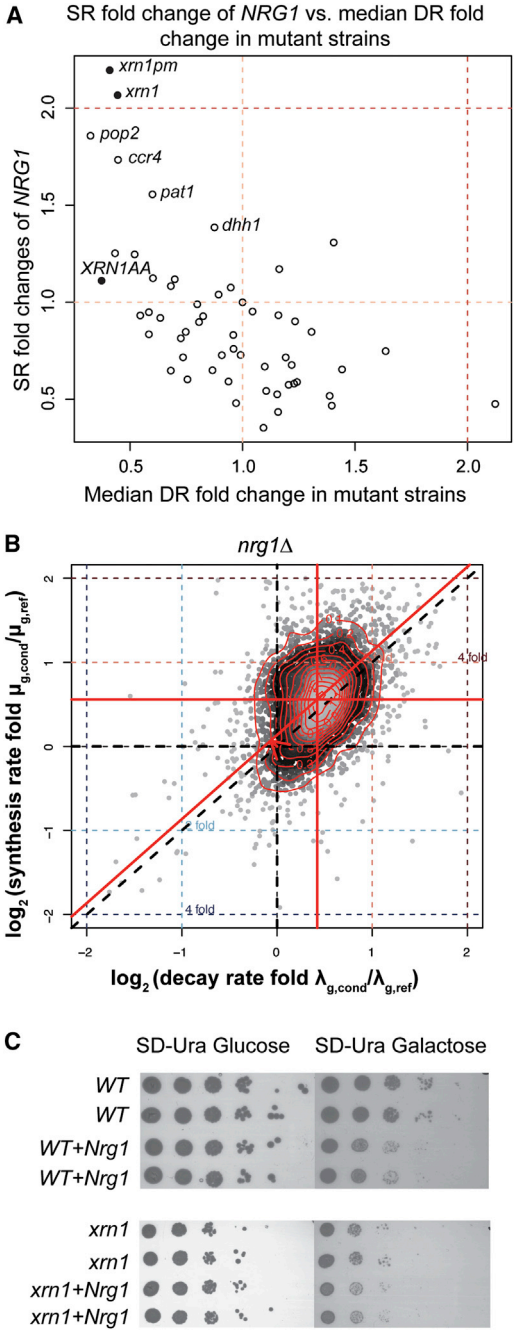

Figure 3. mRNA Level Buffering Involves Transcription Repressor Induction

(A) The SR of the transcription repressor NRG1 is anticorrelated with the median DR of the yeast deletion strains. The x axis represents the median DR fold changes of the strains compared to BY4741. The y axis represents the SR fold changes of the transcription repressor *NRG1* in the strains compared to BY4741.

(B) Scatter plot as in Figure 2 showing DR and SR changes in *nrg1Δ*.

(C) Nrg1 overexpression leads to a slow-growth phenotype. Cultures of wild-type and *xrn1Δ* transformed with *pRS316* or *Gal-NRG1* were grown in SD-URA medium at 30°C overnight and diluted to an OD_{600} of 1 with fresh medium. The same amount of cells was spotted on plates in 10-fold serial dilutions. Plates were incubated for 4 days at 30°C and inspected daily. See also Figure S3.

Xrn1 Represses mRNA Synthesis

To investigate whether the increase in SRs upon deletion of Xrn1 may be due to SR repression by the presence of Xrn1 in the nucleus, we depleted Xrn1 from the nucleus using the anchor-away technique (Haruki et al., 2008) and monitored changes in SR and DR. We generated an Xrn1 anchor-away (*XRN1-AA*) strain in which Xrn1 was fused with a FKBP-rapamycin binding (FRB) domain in a strain containing the ribosomal protein RPL13A fused to the FKBP12 receptor of rapamycin (Haruki et al., 2008). Upon rapamycin addition, the Xrn1-FRB fusion protein was pulled out of the nucleus (not shown). When the *XRN1-AA* strain was grown in media supplemented with rapamycin, the median SR was increased 1.5-fold during mid-log growth phase (Figure 2C), in agreement with a 1.6-fold increase in the *xrn1Δ* strain. The median DR was increased 1.9-fold, possibly due to increased cytoplasmic Xrn1 levels.

These results were consistent with a nuclear function of Xrn1 in repressing mRNA synthesis and with reports that Xrn1 interacts with nuclear proteins such as histones (Gilmore et al., 2012; Lambert et al., 2009) and the Nrd1 complex (Gavin et al., 2006). However, we did not detect association of Xrn1 with the constitutively transcribed genes *ADH1*, *ILV5*, and *RPS11A* by means of chromatin immunoprecipitation (ChIP) in vivo (not shown). Also, Xrn1 was not required for activator- and promoter-dependent transcription in vitro, because nuclear extracts from *xrn1Δ* cells were active in transcription assays (Experimental Procedures, Figure S2). In these assays, addition of TAP-purified Xrn1 protein or the catalytically inactive Xrn1pm variant did not change the activity of transcription. These results indicated that Xrn1 has a nuclear function, but argue against a direct function in mRNA synthesis.

Induction of Transcription Repressor Nrg1

We next searched for nuclear factors that may inhibit mRNA synthesis in an Xrn1-dependent manner. We investigated DR-dependent changes in SRs of transcription repressors. We observed that the SRs for the gene encoding the transcription repressor Nrg1 (Vyas et al., 2005) were increased in the *xrn1Δ* strain and in several other strains with decreased global DR (*xrn1pm*, *ccr4Δ*, *pop2Δ*, *pat1Δ*, *dhh1Δ*; Figure 3A). Vice versa, the SR of NRG1 mRNA was repressed in mutants with increased median DR such as *dcs1Δ* and *rtt103Δ*. The general significance of these changes is revealed by an anticorrelation between changes in SR of NRG1 mRNA with the median DR of the mutant strain (Spearman's correlation −0.61, R^2 = 0.41) (Figure 3A). These results suggested that Nrg1 could be part of the buffering machinery.

To study whether Nrg1 acts globally as a transcription repressor, we collected cDTA data from the *nrg1Δ* deletion strain (Figure 3B). The median SR increased 1.6-fold, as expected for a global transcription repressor, and the DR increased to 1.4-fold. To investigate the relationship between Xrn1 and Nrg1 further, we induced overexpression of Nrg1 in wild-type and *xrn1Δ* mutant yeast cells (Figure 3C). Overexpression of Nrg1 in wild-type cells led to a slow-growth phenotype, as expected for a transcription repressor. However, there was no additive effect observed when Nrg1 was overexpressed in *xrn1Δ* cells, indicating that repression of transcription by Nrg1 requires Xrn1

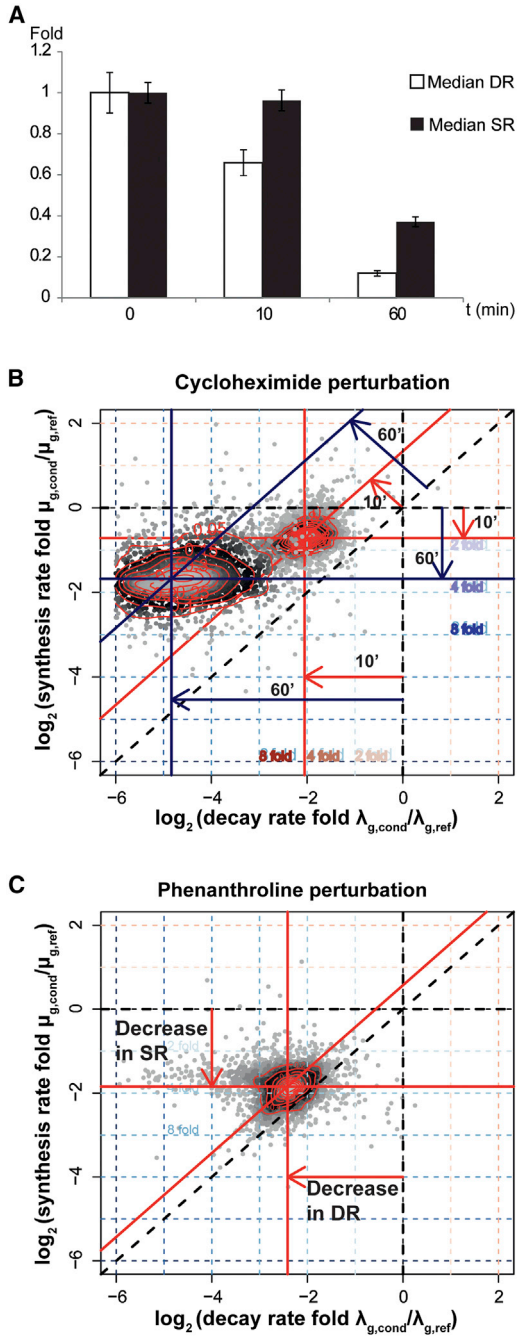

Figure 4. mRNA Level Buffering upon Inhibition of mRNA Degradation or Synthesis

(A) Time-dependent changes in median DRs and SRs upon cycloheximide perturbation. The error bars indicate the standard deviation calculated from the replicate measurements.

(B) Scatter plot comparing changes in SRs (log fold, y axis) and DRs (log fold, x axis) upon degradation inhibition by cycloheximide perturbation in wild-type yeast after 10 min (red lines) and 60 min (blue lines) (depicted as in Figure 2). After 10 min treatment, there is a global shift in the median DR by 0.28-fold and a global shift in the median SR by 0.61-fold. The total mRNA levels change 2.22-fold globally. After 60 min treatment, there is a global shift in the median DR by 0.06-fold and a global shift in the median SR by 0.35-fold. This resulted in a total mRNA level change globally by 2.68-fold. See also Figure S4.

and consistent with the model that Xrn1 is part of the buffering machinery. We also obtained cDTA data from a *nrg1*Δ*xrn1*Δ double deletion strain (Figure S3). The data showed that the DRs decreased to 0.5-fold and SRs decreased to 0.7-fold. Thus, the double mutant phenotype cannot simply be explained by addition of the phenotypes of the individual mutants *nrg1*Δ and *xrn1*Δ. It rather reflects the result of complex changes caused by deletion of two genes. The phenotype may be interpreted as a suppression of the SR phenotype in the *nrg1*Δ background by a reduction of DRs upon Xrn1 deletion and indicates that Nrg1 functions synergistically with Xrn1.

Delayed mRNA Buffering upon Degradation Inhibition

These results suggested that downregulation of mRNA degradation triggers the expression of transcription repressor Nrg1 that subsequently downregulates mRNA synthesis and establishes mRNA level buffering. If true, mRNA level buffering would occur in a time-delayed manner after conditionally impairing mRNA degradation. To test this, we downregulated mRNA degradation with the use of cycloheximide, a translation elongation inhibitor that impairs mRNA degradation (Hu et al., 2009). We added cycloheximide to cells during the mid-log growth phase at a low concentration of 0.1 μg/ml, which has almost no effect on cell growth (Figure S4), suggesting that this concentration does not strongly perturb cellular metabolism. We used cDTA to quantify changes in SRs and DRs after 10 and 60 min of treatment.

The median DR was decreased to 65% after 10 min of cycloheximide treatment and to 12% after 60 min (Figures 4A and 4B). This confirmed the generality of translation-coupled mRNA degradation (Hu et al., 2009). The median SR remained essentially unchanged after 10 min of cycloheximide treatment, but was strongly decreased to about 37% after 60 min (Figures 4A and 4B). This demonstrated that mRNA level buffering occurs in wild-type cells. Remarkably, the SR for Nrg1 mRNA showed a dramatic 7.1-fold increase after 60 min of cycloheximide treatment, in contrast to the general decrease in SRs observed for most mRNAs. These results demonstrate time-delayed mRNA level buffering and synthesis induction of transcription repressor Nrg1 upon inhibition of mRNA degradation and are consistent with an indirect role of Xrn1 in the buffering mechanism.

Rapid Buffering upon mRNA Synthesis Inhibition

The above results indicated that mRNA level buffering following impaired mRNA degradation is delayed, due to transcription repressor induction. To test whether mRNA buffering following impaired mRNA synthesis is also delayed, we treated wild-type cells with 1,10-phenanthroline, an inhibitor of mRNA synthesis, and monitored changes in SRs and DRs. We added 1,10-phenanthroline to cells at mid-log growth at a concentration of 25 μg/ml, which is typically used to arrest transcription (Dori-Bachash et al., 2012), and carried out cDTA after 18 min of

(C) Scatter plot as in (B) but upon mRNA synthesis inhibition by phenanthroline perturbation after 18 min. There is a global shift in the median DR by 0.29-fold, and in the median SR by 0.378-fold. The total mRNA levels are essentially unchanged.

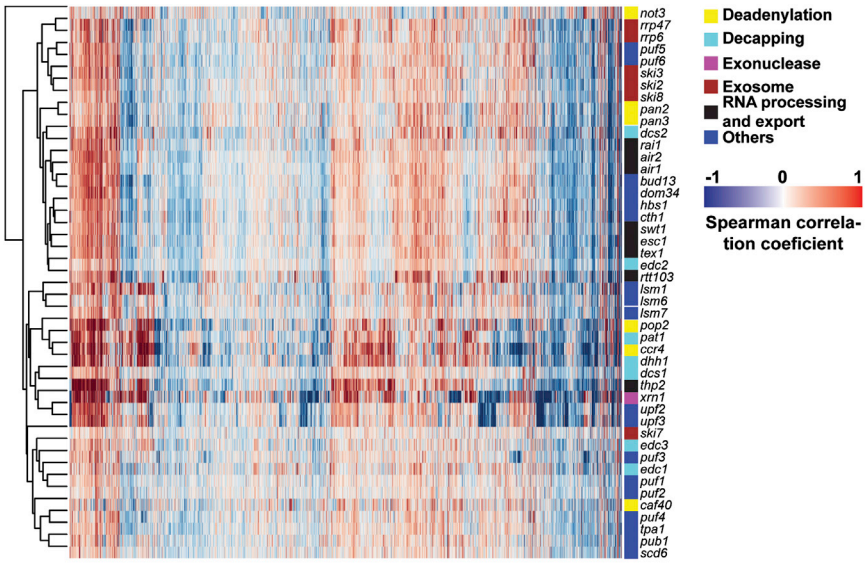

Figure 5. Cluster Analysis of DR Profiles of the 46 Deletion Strains

The pairwise Spearman correlation was used for average-linkage, Euclidean distance-based hierarchical clustering of the mutants (rows) and 2761 genes (columns) with highest variance (>0.01). The color code indicates DR changes from red (increased DR) to blue (decreased DR).

treatment. The median SR was decreased to 38% of the untreated level, as expected after transcription inhibitor treatment (Figure 4C). The median DR was also strongly decreased to 29% after 18 min. This demonstrated that conditional inhibition of mRNA synthesis leads to a rapid decrease in mRNA degradation rates and mRNA level buffering.

Cluster Analysis Reveals mRNA Degradation Complexes

Our data provide a wealth of information on interactions between mRNA degradation factors and on their general and gene-specific functions (Figures 5 and 6). Cluster analysis of the mutant strains based on their DR changes (Figures 5 and 6A) was translated into a two dimensional network plot (Figure 6B), in which the distances between nodes are given by the Spearman correlation coefficient ($R > 0.5$). This revealed known functional relationships between factors. Mutants cluster together when they lack subunits of a known physical protein complex, such as the Ccr4-Not complex (Ccr4 and Pop2 Spearman correlation coefficient, $R = 0.67$), the Lsm complex (Lsm1, Lsm6, and Lsm7, $R > 0.5$), the Ski complex (Ski2, Ski3m and Ski8, $R > 0.62$), the exosome (Rrp6 and Rrp47, $R = 0.75$), components in the TRAMP complex, the zinc-knuckle orthologs Air1 and Air2 ($R = 0.66$), the No-Go mRNA decay complex (Hbs1 and Dom34, $R = 0.67$) (Becker et al., 2011), and the UPF-EJC complex involved in nonsense-mediated decay (NMD) (Upf2 and Upf3, $R = 0.80$). Factors with similar cellular functions build up subclusters, such as the deadenylase subunits Pan2 and Pan3 ($R = 0.78$) and the decapping enchancers Dhh1 and Pat1 ($R = 0.70$). Cluster analysis also recovers known genetic interactions between factors, for example between Swt1, Ecs1, and Tex1 ($R > 0.60$) (Skruzný et al., 2009) (Figures 5 and 6B). Thus, the cluster analysis reliably reveals known interactions between degradation factors in functional complexes and can be used to detect novel interactions.

General mRNA Degradation Machinery

We observe correlations of DR changes in strains with deletions of the Ccr4-Not complex subunits, Xrn1, Pat1, Dhh1, and the Lsm complex (Figure 6 and Figure S5). This indicates that the general mRNA degradation machinery that has been identified biochemically is responsible for global mRNA turnover and comprises the Ccr4-Not deadenylase complex, the Xrn1 5′-exonuclease, and the decapping activator Pat1 and thus, apparently, the decapping complex Dcp1-Dcp2, which we could not include in our analysis due to its essential nature. Our cluster analysis additionally indicates that the THO transcription elongation complex and the scavenger decapping factor Dcs2 are components of a general degradation machinery. The Ski complex subunits Ski2, Ski3, and Ski8 cluster, consistent with formation of a stable complex (Synowsky and Heck, 2008; Wang et al., 2005) that cooperates with the exosome (Araki et al., 2001). In contrast, the Ski7 subunit deletion results in a different profile (Spearman's correlation < 0.15 to Ski2, Ski3, and Ski8), suggesting a peripheral location and functional differences for this subunit (Araki et al., 2001). The three Edc proteins apparently have gene-specific functions.

Deadenylase Complexes Differ in Substrate Preference

The cluster analysis also reveals differences between the two mRNA deadenylase complexes Ccr4-Not and Pan2-Pan3. Deletion of Ccr4-Not complex subunits leads to strong degradation defects, whereas deletion of Pan2 or Pan3 has mild effects (Figures 1A). In addition, the DR changes are not correlated ($R < 0.05$ between Ccr4 and Pan2/3), indicating different mRNA substrate preferences of the two complexes. The mRNAs that show a decreased DR in *pan2*Δ and *pan3*Δ strains are not strongly influenced by deletion of Ccr4-Not complex subunits, or their DR is even higher (Figure 5 and Figure S5). The deadenylation mechanism may be different in human, where Pan2-Pan3 initiates deadenylation (Boeck et al., 1996; Yamashita et al., 2005), whereas the Ccr4-Not complex degrades most of the pA tail (Bai et al., 1999; Collart, 2003). The analysis further showed that DR changes observed upon deletion of the Caf40 subunit of the Ccr4-Not complex do not correlate with other complex subunits ($R < 0.07$ between Caf40 and Ccr4/Not3), in agreement with a previous description of functional modules in the Ccr4-Not complex (Cui et al., 2008). The analysis also reveals a functional interaction of the Pan2-Pan3 complex with the Tex1 subunit of the TREX complex ($R > 0.55$), which is involved in mRNA export (Strässer et al., 2002).

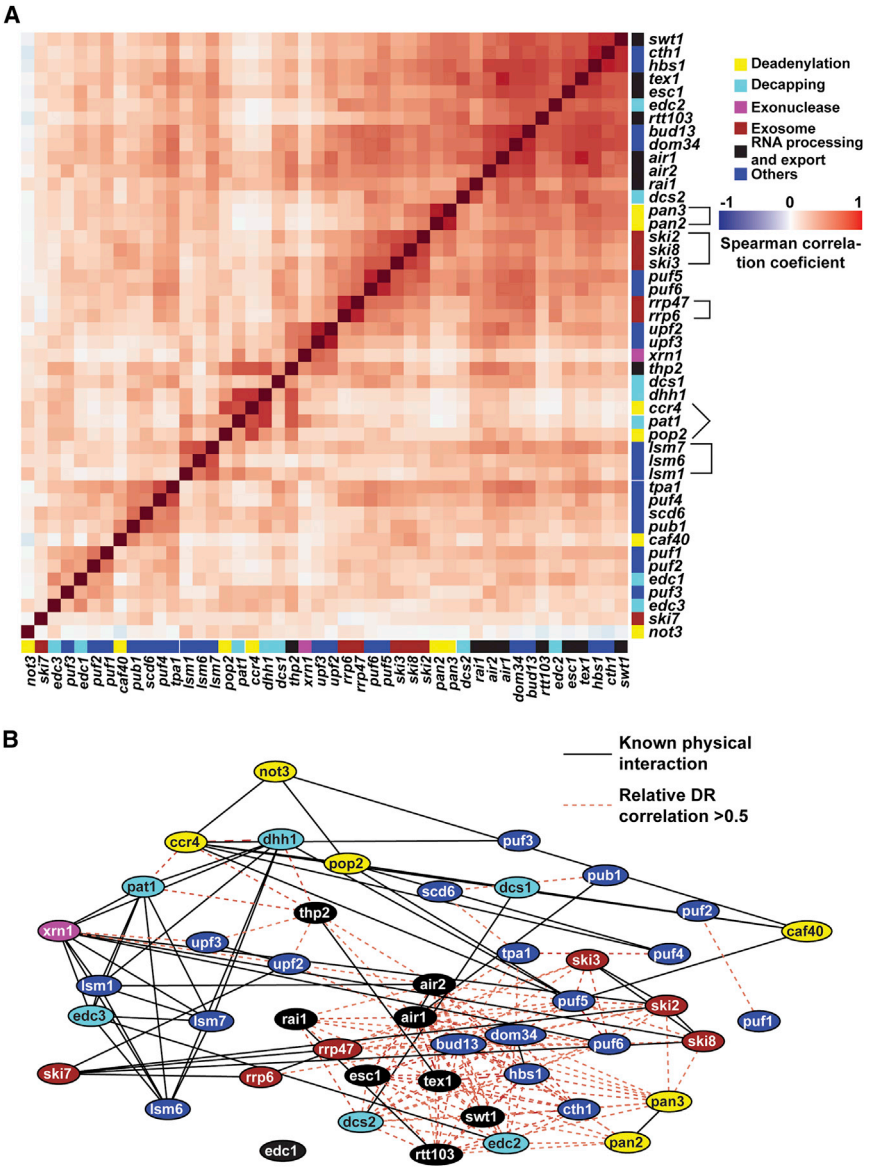

Figure 6. Correlation Analysis of Deletion Strains Reveals Functional Interactions

(A) Correlation analysis of relative DR profiles of the 46 deletion strains. The pairwise Spearman correlation was subjected to hierarchical clustering. The color code gives the value and direction of correlation from strong positive correlation (red) to negative correlation (blue). See also Figure S5.

(B) Two-dimensional network representation of the correlations in (A) (1-Spearman correlation coefficients) used as a distance metric. Proximity of nodes indicates strong positive correlation (Spearman correlation coefficients > 0.5). The black solid lines represent known physical interactions (STRING database) and the red dashed lines represent positive correlations. See also Figure S6.

Scavenger Decapping Factors Dcs1 and Dcs2 Are Global Antagonists

For mRNA molecules that were not decapped but degraded from the 3′ end by the exosome complex, the scavenger decapping enzyme clears up the residual 5′ portion of the RNA (Liu et al., 2002; Muhlrad et al., 1995). Our data show that the *S. cerevisiae* scavenger decapping enzyme Dcs1 and its inhibitor Dcs2 function globally, since all DRs are changed, and that their function is globally antagonistic (Figure S6). In the *dcs1*Δ strain, the median DR is decreased 1.7-fold, whereas it is increased 1.8-fold in the *dcs2*Δ strain (Figure 1A). This is consistent with a general role of Dcs1 in mRNA degradation (Liu and Kiledjian, 2005) and reveals a general role of Dcs2 in inhibiting Dcs1 that is not restricted to stress conditions (Malys and McCarthy, 2006). The DR profiles of *dcs1*Δ and *dcs2*Δ mutant strains were slightly correlated (Figure 6), consistent with the fact that Dcs2 does not contribute to the substrate specificity and only globally represses the enzymatic activity of Dcs1.

An Interwoven mRNA Surveillance Network

In the nucleus, aberrant RNAs are recognized by TRAMP complexes, which add a pA tail to enable exosome-dependent degradation (Vanácová et al., 2005). The subunits Air1 and Air2 are part of two distinct TRAMP complexes and determine the substrate specificity of the nuclear exosome (San Paolo et al., 2009; Schmidt et al., 2012). In the cytoplasm, an mRNA that causes the ribosome to stall is subjected to No-Go decay (Shoemaker and Green, 2012), which involves the factors Dom34 and Hbs1, and mRNAs that contain a nonsense codon are subjected to NMD, which involves the factors Upf2 and Upf3. Aberrant nascent RNAs with an incomplete cap structure are degraded by the 5′-exonuclease Rat1 and its cofactor Rai1 (Schmid and Jensen, 2010). Rai1 and its associated factor Rtt103 cluster with Air1, Air2, Esc1, Tex1, and Bud13 (R > 0.5). This cluster involves the TRAMP-dependent perinuclear mRNP surveillance system (Skruzný et al., 2009), the mRNA export complex (Strässer et al., 2002), and factors involved in pre-mRNA splicing and retention.

Our cluster analysis suggests a functional interaction between Air1-Air2 and Dom34-Hbs1 (R > 0.65) and Upf2-Upf3 (R > 0.46), but factors involved in No-Go decay and NMD do not correlate. Air1-Air2 and Hbs1-Dom34 cluster with Tpa1, a putative translation termination factor (Keeling et al., 2006), indicating Tpa1 as a translation termination factor for No-Go decay. The Tpa1 DR profile resembles those of the polyA-binding protein Pub1 (R = 0.49) and the inhibitor of translation initiation Scd6 (R = 0.51) (Rajyaguru et al., 2012; Ruiz-Echevarría and Peltz, 2000). Surprisingly,

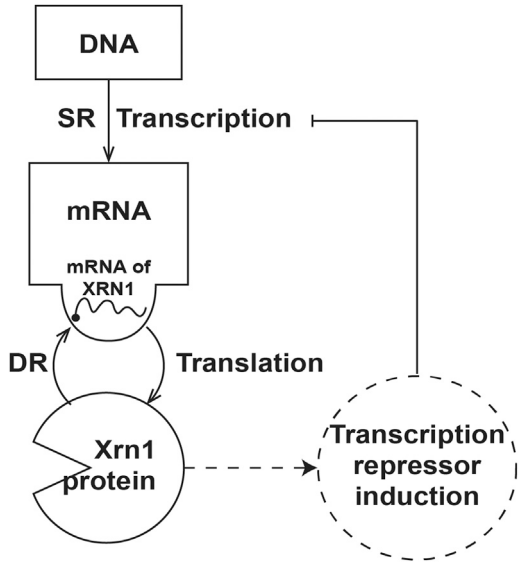

Figure 7. Model for the Cellular Mechanism of mRNA Level Buffering
The mRNA levels are controlled by feedback regulation of XRN1 mRNA levels. Xrn1 protein level is maintained by translation and degradation of XRN1 mRNA. The global SR is controlled by Xrn1-dependent transcription repressor induction.

the mRNA-binding factor Cth1, which belongs to the TIS11 family, plays a role in iron response (Sanvisens et al., 2011), and targets AU-rich elements (Sanduja et al., 2011; Stevens et al., 1998), also shows high correlation to Dom34, Hbs1, and Swt1 ($R > 0.65$), suggesting a role in mRNA surveillance. Upf2 and Upf3 show differences in mRNA substrate preference and cluster with Pub1, which is involved in NMD (Ruiz-Echevarría and Peltz, 2000), and with Puf6, one of six Puf proteins in yeast that have distinct functions (Gerber et al., 2004; Goldstrohm et al., 2007; Miller and Olivas, 2011). These findings suggest a redundant mRNA surveillance system with interconnected activities.

DISCUSSION

We present a global analysis of changes in cellular mRNA synthesis and degradation rates upon deletion of 46 factors involved in eukaryotic mRNA turnover. The significance of the obtained data set is two-fold. First, it demonstrates the generality of mRNA level buffering in a eukaryotic cell and implicates the exonuclease Xrn1 and the transcription repressor Nrg1 in the buffering mechanism. Second, it is a resource providing a wealth of information on the global and gene-specific function of factors involved in mRNA degradation and related processes and the functional interactions between these factors. Our study shows that Xrn1-dependent mRNA level buffering is contributing to the robustness of genome expression and elucidates the mechanisms underlying this phenomenon.

Our results suggest a simple model that may explain mRNA level buffering (Figure 7). A simple feedback loop may link the level of Xrn1 mRNA with its product, the Xrn1 exonuclease protein. When Xrn1 mRNA levels rise, Xrn1 protein levels rise, leading to a subsequent decrease of its mRNA levels. When Xrn1 mRNA levels fall, Xrn1 protein levels fall, leading to mRNA stabilization and thus an increase of the mRNA level. Since Xrn1 acts globally on all mRNA, this simple feedback loop can control all mRNA levels.

The model also explains mRNA level buffering upon perturbation. When mRNA synthesis is impaired, Xrn1 mRNA and protein levels decrease, leading to slower global mRNA degradation. When mRNA degradation is impaired, transcription repressors such as Nrg1 are induced, leading to a time-delayed downregulation of mRNA synthesis. Transcription repression involves a nuclear function of Xrn1, since Xrn1 deletion or nuclear depletion lead to induction of Nrg1, but not to complete mRNA level buffering. It is likely that the C-terminal region of Xrn1 outside the catalytic domain (Chang et al., 2011) is responsible for this function, because its overexpression inhibits cell growth (Page et al., 1998).

The model apparently requires that Xrn1 levels control decapping, because otherwise nonfunctional decapped messages would accumulate during mRNA level buffering. Such Xrn1-dependent decapping is consistent with genetic and physical interactions of Xrn1 with the Dcp1/2 complex and the decapping activators Lsm1-7 and Pat1 (Bouveret et al., 2000; Braun et al., 2012; Hatfield et al., 1996; Nissan et al., 2010), with colocalization of these proteins (Parker and Sheth, 2007), and with the recent demonstration that Xrn1 interacts with decapping activators (Braun et al., 2012). Xrn1 may thus act as a universal sensor of cellular mRNA levels that controls homeostatic mRNA level maintenance.

While our manuscript was in revision, an independent study was published that also observed that mutation of mRNA degradation factors is compensated by a decrease in transcription (Haimovich et al., 2013), consistent with our findings here and with our earlier publication (Sun et al., 2012). The new paper also reaches the conclusion that Xrn1 is important for mRNA synthesis-degradation compensation. However, inconsistent with our cDTA results, the authors reported that SRs were decreased in a *xrn1*Δ strain and more severely in a catalytically inactive $xrn1^{D208A}$ strain. This discrepancy may be due to the ChIP method used by the authors to approximate SR, which measures gene occupancy with polymerase, but not SR. In contrast, our cDTA protocol directly measures SRs by nonperturbing metabolic labeling of RNA. cDTA also allows for normalization between strains and thus the detection of global changes in SRs, which is very difficult in ChIP experiments.

In addition to these insights, interactions between factors involved in mRNA metabolism were detected by cluster analysis of our data. This defined a general mRNA degradation machinery that acts globally and apparently includes the Ccr4-Not complex, the Dcp2 decapping machinery, Xrn1, and the exosome, consistent with a large body of published results (Harigaya and Parker, 2012). Cluster analysis also confirmed many known interactions between degradation factors in functional complexes and revealed new functional interactions between factors. New findings include mRNA substrate preferences for the deadenylase complexes Ccr4-Not and Pan2-Pan3 and their putative interaction with the two decapping scavenger proteins that act antagonistically. The data also indicate an involvement of Esc1, Puf1, Cth1, and Swt1 in nuclear mRNA

surveillance, of Cth1 and Swt1 in No-Go decay, and of Tpa1, Pub1, and Puf6 in NMD.

EXPERIMENTAL PROCEDURES

Yeast Strains

Strains used in this study are listed in Table S1. Yeast knockout strains were purchased from the YKO library (Thermo Scientific) or generated by substituting the target gene for a KanMX cassette using homologous recombination in the same genetic background (Longtine et al., 1998). All knockout strains were validated by selective growth on G418 plates and PCR. The validated strains were stored in 50% glycerol at −80°C. Because some of the strains were genetically unstable, they were not maintained on solid culture. For microarray analysis, strains were always directly streaked out on YPD-rich media from glycerol stocks and incubated at 30°C. The strain *XRN1-AA* was generated by substituting the *XRN1* ORF of a PCR product constructed on plasmid (Haruki et al., 2008). The isogenic parental strain Y40343 for anchor-away experiment was from EUROSCARF. The *xrn1pm* strain is generated by transforming the construct containing point mutation into the *xrn1Δ* strain (Weiner and Costa, 1994, Longtine et al., 1998). For overexpression, a plasmid encoding *NRG1* under the control of the Gal1 promoter was purchased from Thermo Scientific and transformed into BY4741 after validation.

FACS Analysis

Twenty milliliters of YPD was inoculated with a saturated overnight culture and incubated at 30°C until OD_{600} reached 0.8. Then a 1 ml sample was taken and 2.5 ml ethanol was added. Cells were then washed with 50 mM sodium citrate (pH 7.0), and RNA was digested at 37°C overnight with 0.1 mg/ml RNase A (Fermentas). Cells were washed with citrate buffer and subjected to protease K digestion at 50°C for 2 hr. After washing, cells were resuspended in 50 mM sodium citrate buffer containing 1 μM Sytox Green (Invitrogen). To avoid cell clustering, we sonified cells four times for 30 s in a Biorupter (DIAGENODE). The measurement was carried out on a BD FACSCalibur machine. The data were analyzed use the FCS Express software (De Novo Software).

cDTA and Perturbation Assays

cDTA was carried out as described (Sun et al., 2012). *S. cerevisiae* cultures were grown at 30°C in 50 ml aliquots of YPD medium. *S. pombe* cultures were grown at 32°C in YES medium. For inhibitor perturbation, BY4741 cells (OD_{600} = 0.1) were inoculated from a saturated overnight culture in two 100 ml aliquots of YPD liquid medium, incubated at 30°C and grown to early-log phase (OD_{600} = 0.8). Cells were labeled for 6 min (sample 0 min). Then cycloheximide was added and cells were labeled for 10 min and 60 min. Cells were harvested and treated as described (Sun et al., 2012). 1,10-Phenanthroline was added to the culture to a final concentration of 25 μg/ml as described (Dori-Bachash et al., 2012) and labeled for 6 min after 18 min treatment. Cells were treated as above. For the anchor-away analysis, *S. cerevisiae* cells (OD_{600} = 0.1) were cultured in two 200 ml aliquots of YPD containing 1 μg/ml rapamycin and incubated at 30°C until OD_{600} reached 0.8. Due to the instability of rapamycin, we added 1 μg/ml rapamycin every 2 hr. Then a 20 ml sample was taken and labeled with 4sU (Haruki et al., 2008). The cells were then treated as described (Sun et al., 2012).

cDTA Data Analysis

Data was processed with R/Bioconductor as described (Sun et al., 2012). We used a custom probe annotation environment (cdf) to exclude cross-hybridizing probes from further analysis. Labeling bias estimation and correction was performed as described (Miller et al., 2011). Interarray normalization of arrays containing mixed *S. cerevisiae* and *S. pombe* total and labeled RNA was accomplished by proportional rescaling as described (Sun et al., 2012). Samples gained with different batches of prelabeled *S. pombe* RNA were adjusted according to their respective wild-type reference by proportional rescaling. *S. cerevisiae* RNA levels were consequently compared on an absolute level. DRs and SRs were obtained as described in the Supplemental Experimental Procedures of Miller et al. (2011). The whole analysis workflow has been carried out using the open source R/Bioconductor package DTA (Schwalb et al., 2012).

In Vitro Transcription Assay

Nuclear extracts of *BY4741* and *xrn1Δ* were prepared from 3L yeast culture as described (Ranish et al., 1999; Seizl et al., 2011b). Endogenous Xrn1 and xrn1pm were purified from 4L C-terminally TAP-tagged strains using protein A-coupled IgG-Dynabeads. Activator-dependent in vitro transcription assays were carried out using 200 ng recombinant full-length Gcn4 (Seizl et al., 2011a). The transcript was detected by primer extension using the 5′-Cy5-labeled oligonucleotide 5′-TTCACCAGTGAGACGGGCAAC-3′ (Seizl et al., 2011b). The resulting gel was scanned on a typhoon scanner FLA9400, and the data were analyzed with ImageQuant Software (GE Healthcare).

ACCESSION NUMBERS

Data for this paper have been deposited in ArrayExpress under number E-MTAB-1525.

SUPPLEMENTAL INFORMATION

Supplemental Information includes six figures and five tables and can be found with this article online at http://dx.doi.org/10.1016/j.molcel.2013.09.010.

ACKNOWLEDGMENTS

We thank members of the Tresch and Cramer laboratories. A.T. was supported by the LMU*excellent* guest professorship "Computational Biochemistry." P.C. was supported by the Deutsche Forschungsgemeinschaft (SFB646, TR5, SFB960, GRK1721, CIPSM, NIM), an Advanced Investigator Grant of the European Research Council, the LMU*innovativ* project Bioimaging Network (BIN), the Jung-Stiftung, and the Vallee Foundation.

Received: March 13, 2013
Revised: June 30, 2013
Accepted: September 6, 2013
Published: October 10, 2013

REFERENCES

Araki, Y., Takahashi, S., Kobayashi, T., Kajiho, H., Hoshino, S.-i., and Katada, T. (2001). Ski7p G protein interacts with the exosome and the Ski complex for 3′-to-5′ mRNA decay in yeast. EMBO J. *20*, 4684–4693.

Bai, Y., Salvadore, C., Chiang, Y.-C., Collart, M.A., Liu, H.-Y., and Denis, C.L. (1999). The CCR4 and CAF1 proteins of the CCR4-NOT complex are physically and functionally separated from NOT2, NOT4, and NOT5. Mol. Cell. Biol. *19*, 6642–6651.

Becker, T., Armache, J.-P., Jarasch, A., Anger, A.M., Villa, E., Sieber, H., Motaal, B.A., Mielke, T., Berninghausen, O., and Beckmann, R. (2011). Structure of the no-go mRNA decay complex Dom34-Hbs1 bound to a stalled 80S ribosome. Nat. Struct. Mol. Biol. *18*, 715–720.

Boeck, R., Tarun, S., Jr., Rieger, M., Deardorff, J.A., Müller-Auer, S., and Sachs, A.B. (1996). The yeast Pan2 protein is required for poly(A)-binding protein-stimulated poly(A)-nuclease activity. J. Biol. Chem. *271*, 432–438.

Bouveret, E., Rigaut, G., Shevchenko, A., Wilm, M., and Séraphin, B. (2000). A Sm-like protein complex that participates in mRNA degradation. EMBO J. *19*, 1661–1671.

Braun, J.E., Truffault, V., Boland, A., Huntzinger, E., Chang, C.-T., Haas, G., Weichenrieder, O., Coles, M., and Izaurralde, E. (2012). A direct interaction between DCP1 and XRN1 couples mRNA decapping to 5′ exonucleolytic degradation. Nat. Struct. Mol. Biol. *19*, 1324–1331.

Bregman, A., Avraham-Kelbert, M., Barkai, O., Duek, L., Guterman, A., and Choder, M. (2011). Promoter elements regulate cytoplasmic mRNA decay. Cell *147*, 1473–1483.

Chang, J.H., Xiang, S., Xiang, K., Manley, J.L., and Tong, L. (2011). Structural and biochemical studies of the 5′→3′ exoribonuclease Xrn1. Nat. Struct. Mol. Biol. *18*, 270–276.

Chowdhury, A., Mukhopadhyay, J., and Tharun, S. (2007). The decapping activator Lsm1p-7p-Pat1p complex has the intrinsic ability to distinguish between oligoadenylated and polyadenylated RNAs. RNA *13*, 998–1016.

Collart, M.A. (2003). Global control of gene expression in yeast by the Ccr4-Not complex. Gene *313*, 1–16.

Coller, J., and Parker, R. (2004). Eukaryotic mRNA decapping. Annu. Rev. Biochem. *73*, 861–890.

Coller, J., and Parker, R. (2005). General translational repression by activators of mRNA decapping. Cell *122*, 875–886.

Cui, Y., Ramnarain, D.B., Chiang, Y.-C., Ding, L.-H., McMahon, J.S., and Denis, C.L. (2008). Genome wide expression analysis of the CCR4-NOT complex indicates that it consists of three modules with the NOT module controlling SAGA-responsive genes. Mol. Genet. Genomics *279*, 323–337.

Dori-Bachash, M., Shalem, O., Manor, Y.S., Pilpel, Y., and Tirosh, I. (2012). Widespread promoter-mediated coordination of transcription and mRNA degradation. Genome Biol. *13*, R114.

Dunckley, T., Tucker, M., and Parker, R. (2001). Two related proteins, Edc1p and Edc2p, stimulate mRNA decapping in Saccharomyces cerevisiae. Genetics *157*, 27–37.

Franks, T.M., and Lykke-Andersen, J. (2008). The control of mRNA decapping and P-body formation. Mol. Cell *32*, 605–615.

Garneau, N.L., Wilusz, J., and Wilusz, C.J. (2007). The highways and byways of mRNA decay. Nat. Rev. Mol. Cell Biol. *8*, 113–126.

Gavin, A.-C., Aloy, P., Grandi, P., Krause, R., Boesche, M., Marzioch, M., Rau, C., Jensen, L.J., Bastuck, S., Dümpelfeld, B., et al. (2006). Proteome survey reveals modularity of the yeast cell machinery. Nature *440*, 631–636.

Gerber, A.P., Herschlag, D., and Brown, P.O. (2004). Extensive association of functionally and cytotopically related mRNAs with Puf family RNA-binding proteins in yeast. PLoS Biol. *2*, E79.

Gilmore, J.M., Sardiu, M.E., Venkatesh, S., Stutzman, B., Peak, A., Seidel, C.W., Workman, J.L., Florens, L., and Washburn, M.P. (2012). Characterization of a highly conserved histone related protein, Ydl156w, and its functional associations using quantitative proteomic analyses. Mol. Cell. Proteomics *11*, 011544.

Goldstrohm, A.C., Seay, D.J., Hook, B.A., and Wickens, M. (2007). PUF protein-mediated deadenylation is catalyzed by Ccr4p. J. Biol. Chem. *282*, 109–114.

Haimovich, G., Medina, D.A., Causse, S.Z., Garber, M., Millán-Zambrano, G., Barkai, O., Chávez, S., Pérez-Ortín, J.E., Darzacq, X., and Choder, M. (2013). Gene expression is circular: factors for mRNA degradation also foster mRNA synthesis. Cell *153*, 1000–1011.

Harigaya, Y., and Parker, R. (2012). Global analysis of mRNA decay intermediates in *Saccharomyces cerevisiae*. Proc. Natl. Acad. Sci. USA *109*, 11764–11769.

Haruki, H., Nishikawa, J., and Laemmli, U.K. (2008). The anchor-away technique: rapid, conditional establishment of yeast mutant phenotypes. Mol. Cell *31*, 925–932.

Hatfield, L., Beelman, C.A., Stevens, A., and Parker, R. (1996). Mutations in trans-acting factors affecting mRNA decapping in Saccharomyces cerevisiae. Mol. Cell. Biol. *16*, 5830–5838.

Houseley, J., and Tollervey, D. (2009). The many pathways of RNA degradation. Cell *136*, 763–776.

Hu, W., Sweet, T.J., Chamnongpol, S., Baker, K.E., and Coller, J. (2009). Co-translational mRNA decay in Saccharomyces cerevisiae. Nature *461*, 225–229.

Keeling, K.M., Salas-Marco, J., Osherovich, L.Z., and Bedwell, D.M. (2006). Tpa1p is part of an mRNP complex that influences translation termination, mRNA deadenylation, and mRNA turnover in Saccharomyces cerevisiae. Mol. Cell. Biol. *26*, 5237–5248.

Kshirsagar, M., and Parker, R. (2004). Identification of Edc3p as an enhancer of mRNA decapping in Saccharomyces cerevisiae. Genetics *166*, 729–739.

Lambert, J.-P., Mitchell, L., Rudner, A., Baetz, K., and Figeys, D. (2009). A novel proteomics approach for the discovery of chromatin-associated protein networks. Mol. Cell. Proteomics *8*, 870–882.

Lebreton, A., and Séraphin, B. (2008). Exosome-mediated quality control: Substrate recruitment and molecular activity. Biochimica et Biophysica Acta (BBA) *1779*, 558–565.

Liu, H., and Kiledjian, M. (2005). Scavenger decapping activity facilitates 5′ to 3′ mRNA decay. Mol. Cell. Biol. *25*, 9764–9772.

Liu, H., Rodgers, N.D., Jiao, X., and Kiledjian, M. (2002). The scavenger mRNA decapping enzyme DcpS is a member of the HIT family of pyrophosphatases. EMBO J. *21*, 4699–4708.

Longtine, M.S., McKenzie, A., 3rd, Demarini, D.J., Shah, N.G., Wach, A., Brachat, A., Philippsen, P., and Pringle, J.R. (1998). Additional modules for versatile and economical PCR-based gene deletion and modification in *Saccharomyces cerevisiae*. Yeast *14*, 953–961.

Malys, N., and McCarthy, J.E.G. (2006). Dcs2, a novel stress-induced modulator of m7GpppX pyrophosphatase activity that locates to P bodies. J. Mol. Biol. *363*, 370–382.

Miller, M.A., and Olivas, W.M. (2011). Roles of Puf proteins in mRNA degradation and translation. Wiley Interdiscip Rev RNA *2*, 471–492.

Miller, C., Schwalb, B., Maier, K., Schulz, D., Dümcke, S., Zacher, B., Mayer, A., Sydow, J., Marcinowski, L., Dölken, L., et al. (2011). Dynamic transcriptome analysis measures rates of mRNA synthesis and decay in yeast. Mol. Syst. Biol. *7*, 458.

Muhlrad, D., Decker, C.J., and Parker, R. (1994). Deadenylation of the unstable mRNA encoded by the yeast MFA2 gene leads to decapping followed by 5′—>3′ digestion of the transcript. Genes Dev. *8*, 855–866.

Muhlrad, D., Decker, C.J., and Parker, R. (1995). Turnover mechanisms of the stable yeast PGK1 mRNA. Mol. Cell. Biol. *15*, 2145–2156.

Nissan, T., Rajyaguru, P., She, M., Song, H., and Parker, R. (2010). Decapping activators in *Saccharomyces cerevisiae* act by multiple mechanisms. Mol. Cell *39*, 773–783.

Page, A.M., Davis, K., Molineux, C., Kolodner, R.D., and Johnson, A.W. (1998). Mutational analysis of exoribonuclease I from *Saccharomyces cerevisiae*. Nucleic Acids Res. *26*, 3707–3716.

Pai, A.A., Cain, C.E., Mizrahi-Man, O., De Leon, S., Lewellen, N., Veyrieras, J.-B., Degner, J.F., Gaffney, D.J., Pickrell, J.K., Stephens, M., et al. (2012). The contribution of RNA decay quantitative trait loci to inter-individual variation in steady-state gene expression levels. PLoS Genet. *8*, e1003000.

Parker, R., and Sheth, U. (2007). P bodies and the control of mRNA translation and degradation. Mol. Cell *25*, 635–646.

Pérez-Ortín, J.E., de Miguel-Jiménez, L., and Chávez, S. (2012). Genome-wide studies of mRNA synthesis and degradation in eukaryotes. Biochim. Biophys. Acta *1819*, 604–615.

Pilkington, G.R., and Parker, R. (2008). Pat1 contains distinct functional domains that promote P-body assembly and activation of decapping. Mol. Cell. Biol. *28*, 1298–1312.

Rajyaguru, P., She, M., and Parker, R. (2012). Scd6 targets eIF4G to repress translation: RGG motif proteins as a class of eIF4G-binding proteins. Mol. Cell *45*, 244–254.

Ranish, J.A., Yudkovsky, N., and Hahn, S. (1999). Intermediates in formation and activity of the RNA polymerase II preinitiation complex: holoenzyme recruitment and a postrecruitment role for the TATA box and TFIIB. Genes Dev. *13*, 49–63.

Ruiz-Echevarría, M.J., and Peltz, S.W. (2000). The RNA binding protein Pub1 modulates the stability of transcripts containing upstream open reading frames. Cell *101*, 741–751.

San Paolo, S., Vanacova, S., Schenk, L., Scherrer, T., Blank, D., Keller, W., and Gerber, A.P. (2009). Distinct roles of non-canonical poly(A) polymerases in RNA metabolism. PLoS Genet. *5*, e1000555.

Sanduja, S., Blanco, F.F., and Dixon, D.A. (2011). The roles of TTP and BRF proteins in regulated mRNA decay. Wiley Interdiscip Rev RNA *2*, 42–57.

Sanvisens, N., Bañó, M.C., Huang, M., and Puig, S. (2011). Regulation of ribonucleotide reductase in response to iron deficiency. Mol. Cell *44*, 759–769.

Schmid, M., and Jensen, T.H. (2010). Nuclear quality control of RNA polymerase II transcripts. Wiley Interdiscip Rev RNA *1*, 474–485.

Schmidt, K., Xu, Z., Mathews, D.H., and Butler, J.S. (2012). Air proteins control differential TRAMP substrate specificity for nuclear RNA surveillance. RNA *18*, 1934–1945.

Schwalb, B., Schulz, D., Sun, M., Zacher, B., Dümcke, S., Martin, D.E., Cramer, P., and Tresch, A. (2012). Measurement of genome-wide RNA synthesis and decay rates with Dynamic Transcriptome Analysis (DTA). Bioinformatics *28*, 884–885.

Seizl, M., Hartmann, H., Hoeg, F., Kurth, F., Martin, D.E., Söding, J., and Cramer, P. (2011a). A conserved GA element in TATA-less RNA polymerase II promoters. PLoS ONE *6*, e27595.

Seizl, M., Larivière, L., Pfaffeneder, T., Wenzeck, L., and Cramer, P. (2011b). Mediator head subcomplex Med11/22 contains a common helix bundle building block with a specific function in transcription initiation complex stabilization. Nucleic Acids Res. *39*, 6291–6304.

Shalem, O., Dahan, O., Levo, M., Martinez, M.R., Furman, I., Segal, E., and Pilpel, Y. (2008). Transient transcriptional responses to stress are generated by opposing effects of mRNA production and degradation. Mol. Syst. Biol. *4*, 223.

Shalem, O., Groisman, B., Choder, M., Dahan, O., and Pilpel, Y. (2011). Transcriptome kinetics is governed by a genome-wide coupling of mRNA production and degradation: a role for RNA Pol II. PLoS Genet. *7*, e1002273.

Shoemaker, C.J., and Green, R. (2012). Translation drives mRNA quality control. Nat. Struct. Mol. Biol. *19*, 594–601.

Shyu, A.-B., Wilkinson, M.F., and van Hoof, A. (2008). Messenger RNA regulation: to translate or to degrade. EMBO J. *27*, 471–481.

Skruzný, M., Schneider, C., Rácz, A., Weng, J., Tollervey, D., and Hurt, E. (2009). An endoribonuclease functionally linked to perinuclear mRNP quality control associates with the nuclear pore complexes. PLoS Biol. *7*, e8.

Solinger, J.A., Pascolini, D., and Heyer, W.-D. (1999). Active-site mutations in the Xrn1p exoribonuclease of Saccharomyces cerevisiae reveal a specific role in meiosis. Mol. Cell. Biol. *19*, 5930–5942.

Stevens, C.J., Schipper, H., Samallo, J., Stroband, H.W., and te Kronnie, T. (1998). Blastomeres and cells with mesendodermal fates of carp embryos express cth1, a member of the TIS11 family of primary response genes. Int. J. Dev. Biol. *42*, 181–188.

Strässer, K., Masuda, S., Mason, P., Pfannstiel, J., Oppizzi, M., Rodriguez-Navarro, S., Rondón, A.G., Aguilera, A., Struhl, K., Reed, R., and Hurt, E. (2002). TREX is a conserved complex coupling transcription with messenger RNA export. Nature *417*, 304–308.

Sun, M., Schwalb, B., Schulz, D., Pirkl, N., Etzold, S., Larivière, L., Maier, K.C., Seizl, M., Tresch, A., and Cramer, P. (2012). Comparative dynamic transcriptome analysis (cDTA) reveals mutual feedback between mRNA synthesis and degradation. Genome Res. *22*, 1350–1359.

Synowsky, S.A., and Heck, A.J.R. (2008). The yeast Ski complex is a hetero-tetramer. Protein Sci. *17*, 119–125.

Trcek, T., Larson, D.R., Moldón, A., Query, C.C., and Singer, R.H. (2011). Single-molecule mRNA decay measurements reveal promoter- regulated mRNA stability in yeast. Cell *147*, 1484–1497.

Vanácová, Š., Wolf, J., Martin, G., Blank, D., Dettwiler, S., Friedlein, A., Langen, H., Keith, G., and Keller, W. (2005). A new yeast poly(A) polymerase complex involved in RNA quality control. PLoS Biol. *3*, e189.

Vyas, V.K., Berkey, C.D., Miyao, T., and Carlson, M. (2005). Repressors Nrg1 and Nrg2 regulate a set of stress-responsive genes in Saccharomyces cerevisiae. Eukaryot. Cell *4*, 1882–1891.

Wang, L., Lewis, M.S., and Johnson, A.W. (2005). Domain interactions within the Ski2/3/8 complex and between the Ski complex and Ski7p. RNA *11*, 1291–1302.

Weiner, M.P., and Costa, G.L. (1994). Rapid PCR site-directed mutagenesis. PCR Methods Appl. *4*, S131–S136.

Yamashita, A., Chang, T.-C., Yamashita, Y., Zhu, W., Zhong, Z., Chen, C.-Y.A., and Shyu, A.-B. (2005). Concerted action of poly(A) nucleases and decapping enzyme in mammalian mRNA turnover. Nat. Struct. Mol. Biol. *12*, 1054–1063.